The Fisher–Snedecor $\mathcal{F}$ Distribution: A Simple and Accurate Composite Fading Model

Seong Ki Yoo, *Student Member, IEEE*, Simon L. Cotton, *Senior Member, IEEE*, Paschalis C. Sofotasios, *Senior Member, IEEE*, Michail Matthaiou, *Senior Member, IEEE*, Mikko Valkama, *Senior Member, IEEE*, and George K. Karagiannidis, *Fellow, IEEE*

***Abstract*— We consider the use of the Fisher–Snedecor $\mathcal{F}$ distribution, which is defined as the ratio of two chi-squared variates, to model composite fading channels. In this context, the root-mean-square power of a Nakagami-*m* signal is assumed to be subject to variations induced by an inverse Nakagami-*m* random variable. Comparisons with physical channel data demonstrate that the proposed composite fading model provides as good, and in most cases better, fit to the data compared to the generalized-*K* composite fading model. Motivated by this result, simple novel expressions are derived for the key statistical metrics and performance measures of interest.**

***Index Terms*— Composite fading, inverse Nakagami-*m* distribution, Nakagami-*m* fading, shadowing.**

I. Introduction

THE accurate characterization of fading in propagation channels is essential for understanding and improving the system performance of both conventional and emerging wireless communication systems. Fading is often caused by the interaction of signal components formed by multipath and shadowed signal propagation mechanisms. To encapsulate these effects, various composite fading models have been proposed over the past years [1], [2]. Traditionally, composite fading models have considered a mixture of lognormal shadowing and classical multipath fading models such as Rayleigh, Rice, Nakagami-*m* and Hoyt. However, the main drawback of using the lognormal distribution to model shadowing is that it renders most of the corresponding statistics of interest analytically intractable. To overcome this issue, the gamma distribution has been proposed as an approximation to lognormal distribution to describe shadowing [2].

Manuscript received January 25, 2017; accepted March 9, 2017. Date of publication March 24, 2017; date of current version July 8, 2017. This work was supported in part by the U.K. Engineering and Physical Sciences Research Council under Grant Reference EP/L026074/1, the Department for Employment and Learning Northern Ireland through Grant No. USI080 and the Academy of Finland under Projects 284694 and 288670. The associate by editor coordinating the review of this letter and approving it for publication was G. C. Alexandropoulos. *(Corresponding author: Simon Cotton.)*

S. K. Yoo, S. L. Cotton, and M. Matthaiou are with the Institute of Electronics, Communications and Information Technology, Queen's University Belfast, Belfast BT3 9DT, U.K. (e-mail: syoo02@qub.ac.uk; simon.cotton@qub.ac.uk; m.matthaiou@qub.ac.uk).

P. C. Sofotasios is with the Department of Electronics and Communications Engineering, Tampere University of Technology, 33101 Tampere, Finland, and also with the Department of Electrical and Computer Engineering, Khalifa University, 127788 Abu Dhabi, UAE (e-mail: p.sofotasios@ieee.org).

M. Valkama is with the Department of Electronics and Communications Engineering, Tampere University of Technology, 33101 Tampere, Finland (e-mail: mikko.e.valkama@tut.fi).

G. K. Karagiannidis is with the Department of Electrical and Computer Engineering, Aristotle University of Thessaloniki, 54124 Thessaloniki, Greece (e-mail: geokarag@auth.gr).

Digital Object Identifier 10.1109/LCOMM.2017.2687438

More recently, the inverse gamma distribution was introduced to model the random variation of the mean signal power in composite fading channels [1]. Based on this, we now recall that the square root of a gamma random variable (RV) follows a Nakagami-*m* distribution. Exploiting this property, we consider a composite fading channel, in which the scattered multipath contribution follows a Nakagami-*m* distribution, while the root-mean-square (rms) signal is shaped by an inverse Nakagami-*m* distribution. It is demonstrated that this composite probability density function (PDF) is functionally equivalent to the Fisher-Snedecor $\mathcal{F}$ distribution [3]. We also derive simple expressions for a range of channel related statistics, such as the cumulative distribution function (CDF), moments, moment generating function (MGF) and amount of fading (AF). Novel analytical expressions for the corresponding outage probability (OP) and average bit error probability (ABEP) for the case of binary phase-shift keying (BPSK) and differential phase-shift keying (DPSK) are also obtained.

II. $\mathcal{F}$ Distribution as a Composite Fading Model

A. Signal Model

In an $\mathcal{F}$ composite fading channel, multipath fading is manifested by the same propagation mechanisms responsible for Nakagami-*m* fading whereas, the rms power of the received signal is subject to variation induced by shadowing. Based on this, the composite signal envelope, R, can be defined as $R^2 = \sum_{n=1}^{m} A^2 X_n^2 + A^2 Y_n^2$ where m represents the number of multipath clusters, X_n and Y_n are independent Gaussian RVs, which denote the in-phase and quadrature components of the cluster n, and $\mathbb{E}[X_n] = \mathbb{E}[Y_n] = 0$ and $\mathbb{E}\left[X_n^2\right] = \mathbb{E}\left[Y_n^2\right] = \sigma^2$, with $\mathbb{E}[\cdot]$ denoting statistical expectation. Moreover, A is an inverse Nakagami-*m* RV with the shape parameter m_s and scale parameter, $1/\Omega_s$, set equal to unity (i.e. $\Omega_s = 1$) whose PDF is given by

$$f_A(\alpha) = \frac{2{m_s}^{m_s}}{\Gamma(m_s)\,\alpha^{2m_s+1}} \exp\left(-\frac{m_s}{\alpha^2}\right) \tag{1}$$

where $\Gamma(\cdot)$ denotes the gamma function [4, eq. (8.310.1)].

B. Envelope PDF and CDF

The PDF of the composite signal envelope can be obtained by averaging the infinite integral of the conditional PDF of the Nakagami-*m* process with respect to the random variation of the rms signal power, A, i.e. $f_R(r) = \int_0^\infty f_{R|A}(r|\alpha) f_A(\alpha) \mathrm{d}\alpha$. Using the aforementioned signal model, this insinuates that

$$f_{R|A}(r|\alpha) = \frac{2m^m r^{2m-1}}{\Gamma(m)\,\alpha^{2m}\Omega^m} \exp\left(-\frac{mr^2}{\alpha^2\Omega}\right) \tag{2}$$

where m is the fading severity parameter and $\Omega = \mathbb{E}\left[r^2\right]$ is the mean power. By performing a simple transformation of variables and using [4, eq. (3.326.2)] along with some algebraic manipulations, it follows that

$$f_R(r) = \frac{2m^m (m_s\Omega)^{m_s} r^{2m-1}}{B(m, m_s)(mr^2 + m_s\Omega)^{m+m_s}} \tag{3}$$

where $B(\cdot,\cdot)$ denotes the beta function [4]. The form of the PDF in (3) is functionally equivalent to the $\mathcal{F}$ distribution,[1] where m_s controls the corresponding amount of shadowing of the rms signal power. Thus, as $m_s \to 0$, the rms signal power in $\mathcal{F}$ fading channels undergoes heavy shadowing. Conversely, as $m_s \to \infty$, there is no shadowing of the rms signal power and (3) reduces to the Nakagami-m PDF.

Based on the envelope PDF in (3), the corresponding CDF of the composite signal envelope, $F_R(r) \triangleq \int_0^r f_R(r)\mathrm{d}r$, can be obtained with the aid of [4, eq. (3.194.1)], such that

$$F_R(r) = \frac{m^{m-1} r^{2m}\, {}_2F_1\left(m + m_s, m; m+1; -\frac{mr^2}{m_s\Omega}\right)}{B(m, m_s)(m_s\Omega)^m} \tag{4}$$

where ${}_2F_1(\cdot,\cdot;\cdot;\cdot)$ is the Gauss hypergeometric function [4, eq. (9.111)]. Additionally, the corresponding PDF of the instantaneous SNR, γ, of the $\mathcal{F}$ fading model is also readily obtained by letting $\gamma = \bar{\gamma} R^2/\Omega$, where $\bar{\gamma} = \mathbb{E}\left[\gamma\right]$, yielding

$$f_\gamma(\gamma) = \frac{m^m (m_s\bar{\gamma})^{m_s} \gamma^{m-1}}{B(m, m_s)(m\gamma + m_s\bar{\gamma})^{m+m_s}}. \tag{5}$$

C. Joint Envelope-Phase PDF

Let $Z^2 = \sum_{i=1}^m Z_i^2$, where $Z = AX$ or $Z = AY$ and $Z_i = AX_i$ or $Z_i = AY_i$, as required. As an intermediate step, we find the PDF, $f_W(w)$, of $W = Z^2$ which follows a *chi-square* distribution. The variate Z can be written as $Z = sgn(Z) \times |Z|$ where $sgn(\cdot)$ denotes the sign function and $|Z| = \sqrt{W}$. Consequently, the PDF $f_Z(z)$ of Z can be obtained as follows

$$f_Z(z) = \left(\frac{m}{A^2\Omega}\right)^{\frac{m}{2}} \frac{z^{m-1}}{\Gamma(m/2)} \exp\left(-\frac{mz^2}{A^2\Omega}\right). \tag{6}$$

Using the standard statistical procedure of transformation of variables, we find that $f_{R,\Theta}(r,\theta) = |J| f_{X,Y}(x,y)$ where $|J|$ is the Jacobian of the transformation. By carrying out the required mathematical procedure with $|J| = r$ and $f_{X,Y}(x,y) = f_X(x) f_Y(y)$, we can obtain the conditional PDF of an $\mathcal{F}$ envelope-phase process as follows

$$f_{R|A,\Theta}(r|\alpha,\theta) = \frac{m^m r^{2m-1} |\sin(2\theta)|^{m-1}}{2^{m-1} A^{2m} \Omega^m \Gamma^2(m/2)} \exp\left(-\frac{mr^2}{A^2\Omega}\right). \tag{7}$$

To this effect, the joint envelope-phase PDF of an $\mathcal{F}$ fading process can be obtained using $f_{R,\Theta}(r,\theta) = \int_0^\infty f_{R|A,\Theta}(r|\alpha,\theta) f_A(\alpha)\mathrm{d}\alpha$, which after some algebraic manipulations can be expressed as

$$f_{R,\Theta}(r,\theta) = \frac{m^m (m_s\Omega)^{m_s} \Gamma(m+m_s) r^{2m-1} |\sin(2\theta)|^{m-1}}{2^{m-1}\Gamma(m_s)\Gamma^2(m/2)(mr^2 + m_s\Omega)^{m+m_s}}. \tag{8}$$

Evidently, integrating (8) with respect to r yields the Nakagami-m phase PDF given in [5], as expected.

[1]Letting $r^2 = \Omega t$, $m = d_1/2$, $m_s = d_2/2$ and performing the required transformation yields the $\mathcal{F}$ distribution, $f(t)$, with parameters d_1 and d_2.

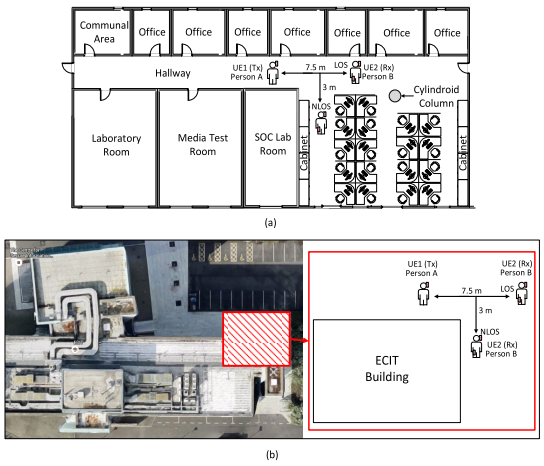

Fig. 1. D2D measurements conducted in (a) the indoor open office area environment and (b) the outdoor open space environment, showing the different locations of person B for the LOS and NLOS channel conditions.

D. Moments and MGF

With the aid of (5), the n^{th} moment of the instantaneous SNR can be derived using [4, eq. (3.194.3)], namely

$$\mathbb{E}\left[\gamma^n\right] = \left(\frac{m_s\bar{\gamma}}{m}\right)^n \frac{B(m+n, m_s-n)}{B(m, m_s)}, \quad m_s > n. \tag{9}$$

Likewise, the MGF of the $\mathcal{F}$ fading model can be derived using the generalized Laguerre polynomials and [4, eq. (3.383.5)]. To this end, after some algebraic manipulations, one obtains

$$M_\gamma(-s) = {}_1F_1\left(m; 1-m_s; \frac{s\bar{\gamma}m_s}{m}\right) + \frac{\Gamma(-m_s)}{B(m, m_s)} \times \left(\frac{s\bar{\gamma}m_s}{m}\right)^{m_s} {}_1F_1\left(m+m_s; 1+m_s; \frac{s\bar{\gamma}m_s}{m}\right), s > 0 \tag{10}$$

which is valid for $m + m_s \neq \mathbb{N}$ and $m_s \neq \mathbb{N}$, while ${}_1F_1(\cdot;\cdot;\cdot)$ denotes the Kummer confluent hypergeometric function [4, eq. (9.210.1)].

III. Empirical Comparison of $\mathcal{F}$ and K_G Models

The usefulness of the $\mathcal{F}$ distribution to model composite fading channels can be verified by comparing its fit to empirical data contrasted with more established models, such as generalized-K (K_G). To compare the two models, we used field measurements obtained at 5.8 GHz for device-to-device (D2D) communications within an indoor open office area and an outdoor environment. To emulate the user equipment (UE), the hardware setup described in [6] was used. In this study, a D2D link was formed between two persons, namely person A, an adult female of height 1.65 m and weight 51 kg, and person B, an adult male of height 1.83 m and weight 73 kg. As shown in Fig. 1, during the D2D measurements, person A held the UE at her left-ear to imitate making a voice call while person B held the UE either at his left-ear or in the right-front pocket of his clothing to mimic carrying a device under two different channel conditions, namely line-of-sight (LOS) and non-LOS (NLOS).

TABLE I

PARAMETER ESTIMATES FOR THE $\mathcal{F}$ AND K_G MODELS FOR ALL OF THE CONSIDERED D2D MEASUREMENTS ALONG WITH THE AIC RANK

D2D links	Indoor Open Office Environment								Outdoor Open Space Environment							
	$\mathcal{F}(m,\Omega,m_s)$				$K_G(m,\alpha,\beta)$				$\mathcal{F}(m,\Omega,m_s)$				$K_G(m,\alpha,\beta)$			
	m	Ω	m_s	Rank	m	α	β	Rank	m	Ω	m_s	Rank	m	α	β	Rank
H2H LOS	1.12	0.70	1.42	**1**	1.39	1.39	0.88	2	1.04	0.63	1.03	2	1.20	1.20	1.09	**1**
H2H NLOS	0.75	1.20	4.27	2	3.62	0.78	1.96	**1**	0.50	0.01	0.99	**1**	0.78	0.50	0.10	2
H2P LOS	0.98	0.79	2.03	**1**	1.05	2.09	0.57	2	0.54	1.56	20.00	**1**	0.54	16.47	0.10	2
H2P NLOS	1.09	0.91	2.25	2	2.39	1.15	1.15	**1**	0.86	0.30	0.50	**1**	0.86	0.86	1.37	2

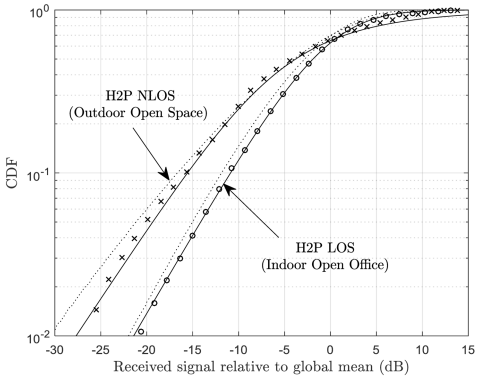

Fig. 2. Comparison of empirical CDFs (symbols) and theoretical CDFs of the $\mathcal{F}$ (continuous lines) and K_G (dotted lines) fading models.

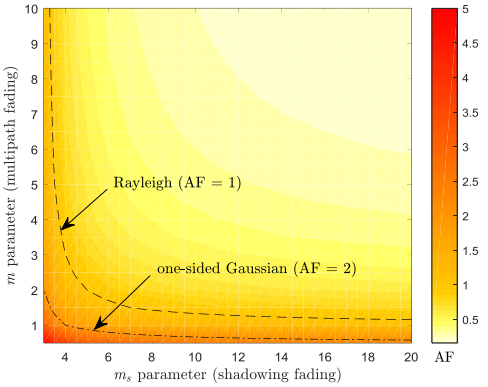

Fig. 3. AF in an $\mathcal{F}$ fading channel as a function of the multipath and shadowed fading parameters.

Consequently, the head-to-head (H2H) and head-to-pocket (H2P) channels were considered in LOS and NLOS conditions for each environment.

The parameter estimates for the $\mathcal{F}$ and K_G fading models were obtained using a non-linear least squares function programmed in MATLAB. To allow our results to be reproduced, all parameter estimates are given in Table I. As an example of data fitting process, Fig. 2 shows the CDFs of the $\mathcal{F}$ and K_G fading models fitted to some empirical data. These plots were typical of the fits obtained, but more importantly illustrated that the characterizations obtained by the $\mathcal{F}$ model provided a better fit to the empirical data at the tail of the CDFs. This is an important attribute of the proposed model as it is the deepest fades which are one of the greatest sources of degradation in wireless system performance. In a similar manner to the analysis performed in [7], here, the Akaike information criterion (AIC) was used to select the most likely model between the $\mathcal{F}$ and K_G distributions. As a result of the ranking performed in Table I (which is based on the computed AIC), it was found that the $\mathcal{F}$ model was selected as the most likely model for 62.5% of the considered cases.

IV. APPLICATIONS IN DIGITAL COMMUNICATIONS

A. Amount of Fading

It is recalled here that the AF is often used as a relative measure of the severity of fading encountered in wireless transmission over fading channels [8]. With the aid of (9), for the case of an $\mathcal{F}$ fading channel, this can be obtained as $\text{AF} = \frac{\mathbb{V}[\gamma]}{\mathbb{E}^2[\gamma]} = \frac{\mathbb{E}[\gamma^2]}{\mathbb{E}^2[\gamma]} - 1 = \frac{m+m_s-1}{m(m_s-2)}$ where $\mathbb{V}[\cdot]$ denotes the variance operator. Fig. 3 shows the estimated AF values for different multipath ($0.5 \leq m \leq 10$) and shadowed fading ($3 \leq m_s \leq 20$) conditions. It is clear that the greatest AF occurs when the channel is subject to simultaneous heavy shadowing ($m_s \to 3$) and severe multipath fading ($m \to 1/2$). On the contrary, the value of the AF approaches zero as both the multipath and shadowed fading parameters become large (i.e. $m, m_s \to \infty$). In particular, when $m_s \to \infty$ this reduces to the AF of a Nakagami-m fading channel, i.e. $\text{AF} = 1/m$, and consequently asymptotically approaches the AF of the Rayleigh (AF = 1) and one-sided Gaussian (AF = 2) models when $m \to 1$ and $m \to 1/2$ respectively.

B. Outage Probability

The OP for the case of $\mathcal{F}$ fading can be derived with the aid of [4, eq. (3.194.1)], as

$$P_{\text{out}} = \frac{m^{m-1}\gamma_{\text{th}}{}^m {}_2F_1\left(m+m_s, m; m+1; -\frac{m\gamma_{\text{th}}}{m_s\bar{\gamma}}\right)}{B(m,m_s)(m_s\bar{\gamma})^m} \quad (11)$$

where γ_{th} is the pre-determined SNR threshold. For the case of asymptotically large values of $\bar{\gamma}$, the OP can be expressed as $P_{\text{out}} = (O_c\bar{\gamma})^{-O_d} + o\left(\bar{\gamma}^{-O_d}\right)$, where O_c and O_d denote the coding gain and diversity gain, respectively [9]. For the case of $\mathcal{F}$ fading channels, we have $O_c = \frac{1}{\gamma_{\text{th}}}\left(\frac{m^{m-1}}{B(m,m_s)m_s{}^m}\right)^{-\frac{1}{m}}$ and $O_d = m$. Recognizing that $B(a,b) = \Gamma(a)\Gamma(b)/\Gamma(a+b)$ and $m^{m-1}/\Gamma(m) = m^m/m!$, this yields

$$P_{\text{out}} = \left(\frac{\gamma_{\text{th}}}{m_s\bar{\gamma}}\right)^m \frac{m^m\Gamma(m+m_s)}{m!\Gamma(m_s)} + o\left(\bar{\gamma}^{-O_d}\right). \quad (12)$$

Fig. 4 illustrates the exact OP for heavy ($m_s = 1/2$), moderate ($m_s = 5$) and light ($m_s = 50$) shadowed fading environments along with the respective asymptotic curve. The simulation results are also shown in Fig. 4 to verify the analytical results. In this case, the data underlying the simulated plots was obtained through the straightforward calculation of the ratio of two gamma random sequences. It is clear that the OP increases rapidly as the shadowing becomes heavier, indicating that the communication performance degrades in

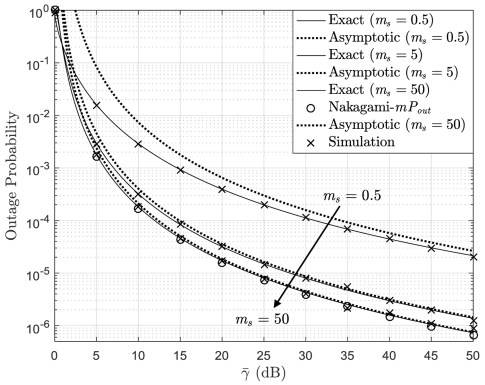

Fig. 4. OP of various $\mathcal{F}$ fading channels considering different shadowed fading conditions for $m = 3.5$ and $\gamma_{\text{th}} = 0.5$.

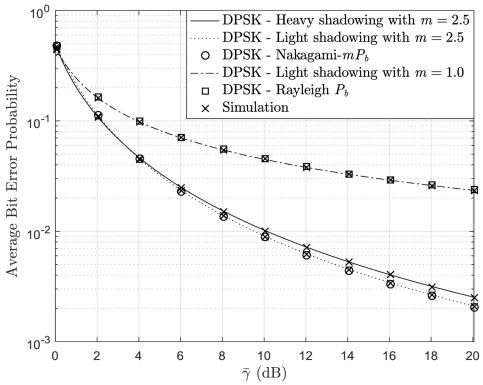

Fig. 5. ABEP of the DPSK modulation scheme for $\mathcal{F}$ fading channels with different levels of shadowed fading.

environments which exhibit heavy shadowed fading characteristics. Moreover, it can be seen that the asymptotic OP provides a good agreement with the exact OP at high average SNR levels. It is also evident that in a lightly shadowed fading environment, the estimated OP for $\mathcal{F}$ distributed channels becomes practically equivalent to the OP of the Nakagami-m channels, namely $P_{\text{out}}^{\text{Nak}} = 1 - \Gamma(m, m\gamma_{\text{th}}/\bar{\gamma})/\Gamma(m)$ [10].

C. Average Bit Error Probability

It is recalled that the ABEP for a DPSK scheme is given by $P_b = c_1 M_\gamma(-c_2)$, in [8, eq. (1.8)], with $c_1 = 1/2$ and $c_2 = 1$. Thus, the ABEP in the case of $\mathcal{F}$ fading channels can be readily deduced using (10). Fig. 5 shows the ABEP versus $\bar{\gamma}$ for DPSK ($c_1 = 0.5$ and $c_2 = 1$) under different multipath and shadowed fading conditions along with the corresponding simulation results. As expected, the ABEP increases rapidly as multipath fading becomes severer and shadowing becomes heavier. Furthermore, in a lightly shadowed fading environment ($m_s = 50$), the estimated ABEP for an $\mathcal{F}$ fading channel approaches the ABEP of Nakagami-m fading channels, where $M_\gamma(s) = (1 - s\bar{\gamma}/m)^{-1}$ [8]. Similarly, by setting $m = 1$ and $m_s = 50$ (light shadowing), the estimated ABEP for an $\mathcal{F}$ fading channel corresponds to that of Rayleigh fading channels, where $M_\gamma(s) = (1 - s\bar{\gamma})^{-1}$ [8].

Recalling the Craig integral representation in [11, eq. (20)], the corresponding ABEP for the case of BPSK modulation can be obtained by substituting (10) into this expression and setting $g = 1$ [12]. Again, it is recalled that for the case of asymptotically large values of $\bar{\gamma}$, $P_E = (G_c\bar{\gamma})^{-G_d} + o\left(\bar{\gamma}^{-G_d}\right)$, where $G_d = m$ and $G_c = u\left(\frac{2^{m-1}m^{m-1}\Gamma(m+1/2)}{\sqrt{\pi}B(m,m_s)m_s{}^m}\right)^{-\frac{1}{m}}$, with u denoting a positive fixed constant which differs according to the chosen modulation scheme, e.g. $u = 2$ for a BPSK scheme. Based on this, a simple asymptotic expression is readily deduced for the ABEP of BPSK modulated signals over $\mathcal{F}$ fading channels

$$P_E = \frac{m^{m-1}\Gamma(m+\frac{1}{2})}{2\sqrt{\pi}B(m,m_s)(m_s\bar{\gamma})^m} + o\left(\bar{\gamma}^{-O_d}\right). \tag{13}$$

V. Conclusion

We have introduced the $\mathcal{F}$ distribution as an accurate and tractable composite model to characterize the combined effects of multipath and shadowing. Using some physical channel data, obtained for D2D communications, it was shown that the $\mathcal{F}$ fading model often provided a better fit compared to the K_G model. Most importantly though, when comparing the analytical forms of the PDFs, CDFs and ABEP of the two models, the $\mathcal{F}$ distribution shows less complexity compared to the K_G model. In particular, the PDF and CDF of the $\mathcal{F}$ distribution require the computation of a smaller number of special functions than the K_G model, while determining the ABEP of the K_G model given in [13, eq. (8)] requires the calculation of the Meijer-G function whereas the ABEP of the $\mathcal{F}$ fading model does not. Based on the tractability of the $\mathcal{F}$ distribution, novel and simple expressions have been derived for the key statistical metrics and performance measures.

References

[1] S. K. Yoo, S. L. Cotton, P. C. Sofotasios, M. Matthaiou, M. Valkama, and G. K. Karagiannidis, "The $\kappa - \mu$ / inverse gamma fading model," in *Proc. IEEE PIMRC*, Aug./Sep. 2015, pp. 527–531.

[2] A. Abdi and M. Kaveh, "K distribution: An appropriate substitute for Rayleigh-lognormal distribution in fading-shadowing wireless channels," *Electron. Lett.*, vol. 34, no. 9, pp. 851–852, Apr. 1998.

[3] C. Walck, "Handbook on statistical distributions for experimentalists," Particle Phys. Group, Fysikum, Univ. Stockholm, Stockholm, Sweden, Tech. Rep. SUF-PFY/96-01, 2007.

[4] I. S. Gradshteyn and I. M. Ryzhik, *Table of Integrals, Series, and Products*, 7th ed. London, U.K.: Academic, 2007.

[5] M. D. Yacoub, G. Fraidenraich, and J. C. S. S. Filho, "Nakagami-m phase-envelope joint distribution," *Electron. Lett.*, vol. 41, no. 5, pp. 259–261, Mar. 2005.

[6] N. Bhargav, S. L. Cotton, and D. E. Simmons, "Secrecy capacity analysis over $\kappa - \mu$ fading channels: Theory and applications," *IEEE Trans. Commun.*, vol. 64, no. 7, pp. 3011–3024, Jul. 2016.

[7] A. Fort, C. Desset, P. De Doncker, P. Wambacq, and L. Van Biesen, "An ultra-wideband body area propagation channel model-from statistics to implementation," *IEEE Trans. Microw. Theory Techn.*, vol. 54, no. 4, pp. 1820–1826, Jun. 2006.

[8] M. K. Simon and M.-S. Alouini, *Digital Communication over Fading Channels*. New York, NY, USA: Wiley, 2005.

[9] Z. Wang and G. B. Giannakis, "A simple and general parameterization quantifying performance in fading channels," *IEEE Trans. Commun.*, vol. 51, no. 8, pp. 1389–1398, Aug. 2003.

[10] N. Yang, M. Elkashlan, and J. Yuan, "Outage probability of multiuser relay networks in Nakagami-m fading channels," *IEEE Trans. Veh. Technol.*, vol. 59, no. 5, pp. 2120–2132, Jun. 2010.

[11] M.-S. Alouini and A. J. Goldsmith, "A unified approach for calculating error rates of linearly modulated signals over generalized fading channels," *IEEE Trans. Commun.*, vol. 47, no. 9, pp. 1324–1334, Sep. 1999.

[12] X. Song, F. Yang, J. Cheng, and M.-S. Alouini, "Asymptotic SER performance comparison of MPSK and MDPSK in wireless fading channels," *IEEE Wireless Commun. Lett.*, vol. 4, no. 1, pp. 18–21, Feb. 2015.

[13] P. S. Bithas, N. C. Sagias, P. T. Mathiopoulos, G. K. Karagiannidis, and A. A. Rontogiannis, "On the performance analysis of digital communications over generalized-K fading channels," *IEEE Commun. Lett.*, vol. 10, no. 5, pp. 353–355, May 2006.